Molecular dynamics modeling of self-diffusion along a triple junction

T. Frolov* and Y. Mishin†
Department of Physics and Astronomy, MSN 3F3, George Mason University, Fairfax, Virginia 22030, USA
(Received 8 December 2008; revised manuscript received 11 March 2009; published 18 May 2009)

We propose a computational procedure for creating a stable equilibrium triple junction (TJ) with controlled grain misorientations. We apply this procedure to construct a TJ between a $\Sigma5(210)$ grain boundary (GB) and two general high-angle GBs in copper and calculate the diffusion coefficients along the TJ and the GBs using molecular dynamics with an embedded-atom potential. The TJ diffusion is only a factor of 2 faster than diffusion in the $\Sigma5$ GB but significantly faster than diffusion in the general GBs. Both the GBs and the TJ studied here show a premelting behavior near the bulk melting point, where their diffusivities converge to the diffusivity of bulk liquid. Although our results are consistent with the common assumption that TJ diffusion is generally faster than GB diffusion, the difference between the two diffusivities does not appear to be large enough to ensure a significant contribution of TJs to diffusional creep in polycrystals at high temperatures.

DOI: 10.1103/PhysRevB.79.174110 PACS number(s): 61.72.Mm, 66.30.Fq, 66.30.Pa

I. INTRODUCTION

The triple junction (TJ) is a line where three grain boundaries (GBs) meet together. It is commonly believed that TJs greatly influence properties of nanocrystalline materials and can play a significant role during plastic deformation and diffusional creep.[1–3]

The TJs are much less-studied crystalline defects than GBs or dislocations are. Experimental investigations of TJs are complicated by many factors, including their high mobility.[4] Experimental measurements indicate that zinc diffusion along TJs in Al is 3 orders of magnitude faster than along GBs.[5] TJs can also be the sites of preferred solute segregation.[6] Some theoretical models introduce the assumption of fast TJ diffusion to explain the anomalous diffusion and deformation behavior of nanocrystalline materials.[3,7,8] However, no reliable experimental information on self-diffusion along TJs is currently available to verify this assumption.

Due to the recent progress in the development of interatomic potentials capturing basic properties of materials on the quantitative level,[9] atomistic simulations offer a means of predicting self-diffusion coefficients that would otherwise be very difficult to measure. For example, the GB self-diffusion coefficients in copper predicted by simulations were found to be in very good agreement with experiment.[10] To the best of our knowledge, TJ diffusion has never been studied by atomistic simulations.

As in experiments, the TJ motion at finite temperatures poses a major challenge to diffusion simulations. In a few studies published so far, the TJ motion was prevented by creating high-symmetry configurations[11] or restricting the simulations to the 0 K temperature. Applying these restrictions, the atomic structure of the TJs at 0 K was carefully examined and their excess energy was estimated;[11,12]; however, no diffusion coefficients were computed. TJ motion by capillary forces at high temperatures has been studied by two-dimensional Lennard-Jones simulations.[13]

In this work, we apply three-dimensional molecular-dynamics (MD) simulations with an embedded-atom potential to compute self-diffusion coefficients along a representative TJ and compare them with self-diffusion coefficient in the adjoining GBs. Since self-diffusion is the only type of diffusion studied here, we will be referring to it for brevity as simply "diffusion." In Sec. II we show how a TJ with controlled grain misorientations can be created in the computer and how its motion can be constrained by boundary conditions. We also introduce our methodology for diffusion calculations. Our results are presented in Sec. III followed by their discussion and conclusions in Sec. IV.

II. METHODOLOGY

We chose copper as the model material, with atomic interactions described by the embedded-atom potential developed in Ref. 14. The same potential was used in the recent study of GB diffusion.[10] The bulk melting point of Cu predicted by this potential is $T_m=1327$ K (the experimental value is 1356 K).

Our procedure for constructing an equilibrium TJ is illustrated in Fig. 1. First, a symmetrical tilt $\Sigma5(210)$ boundary was created with the tilt axis parallel to the common [100] direction of both grains. The grain dimensions are $85\times83\times66$ Å^3, where the third number is the dimension normal to the page. The GB was terminated at a free surface perpendicular to the tilt axis. Another $116\times66\times66$ Å^3 grain with the orientation shown in Fig. 1 was placed on the surface, forming a nonequilibrium TJ. The model was equilibrated by a 2-ns-long MD run at 1100 K with a periodic boundary condition parallel to the TJ and fixed boundary conditions at the bottom and the sides of the block (the top side is exposed to vacuum). The fixed layers shown in Fig. 1 in gray were 10 Å thick. Further details of the MD methodology will be discussed later.

During the MD anneal, the TJ quickly (within the first 0.1 ns) moved down, causing migration of the two initially horizontal GBs until an equilibrium configuration was reached. The planes of the moving GBs changed in this process, but the grain misorientation remained the same. The new GB planes were symmetrical with respect to the $\Sigma5$ GB by construction, but they did not align with any particular low-

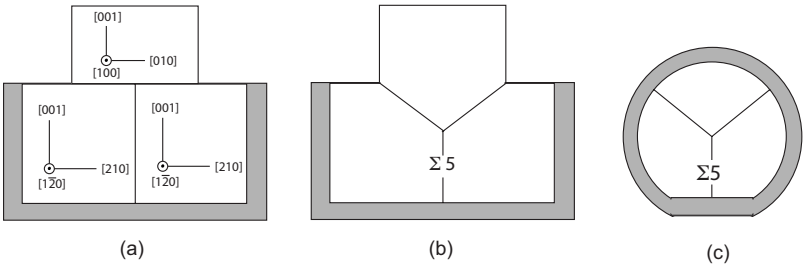

FIG. 1. Schematic showing the procedure for the creation of a TJ. (a) Three grains are joined together by putting a third grain on top of a bicrystal. (b) An equilibrium TJ forms during MD run at a high temperature. (c) A cylindrical region containing the TJ is cut out of the tricrystal and additionally equilibrated. The shaded areas represent fixed atoms.

index crystal planes in the grains. These new boundaries will be referred to as general GBs (GGBs).

Once equilibrated, the TJ and the GBs did not move except for small thermal fluctuations. Note that the $\Sigma 5$ GB is pinned by the fixed region at the bottom, while the GGBs are pinned by the surface grooves formed in the corners between the third grain and the two initial grains.

Finally, a cylindrical region with the axis parallel to the TJ was cut out of the tricrystal [Fig. 1(c)]. The atoms within a 10-Å-thick outer shell of the cylinder were made fixed, whereas all atoms inside the shell were allowed to move during the subsequent MD simulations. The fixed shell served to pin the GBs and prevent their migration. Note that the cross section of the shell is not perfectly circular. It contains the previously formed surface grooves and a portion of the bottom fixed layer from the original block. The boundary condition parallel to the TJ remained periodic. This cylindrical block contained 81 137 atoms and had the length of 66 Å. It was used as initial configurations for the diffusion calculations.

The MD simulations were performed in the *NVT* (canonical) ensemble using a Nose-Hoover thermostat. The integration of the equations of motion employed the Verlet algorithm with the integration time step of 2 fs. The simulations covered the temperature range from 700 (the lowest temperature of reliable diffusion calculations accessible with our computational resources) to 1315 K (12 K below T_m). Prior to an MD run, the block was uniformly expanded/contracted according to the thermal-expansion factor at the intended simulation temperature, using the thermal-expansion factors computed in Ref. 14. The model was then additionally equilibrated by a 1-ns-long MD run to approach the equilibrium point-defect concentrations at the chosen temperature followed by a 10-ns-long production run for diffusion calculations. As a test of equilibration, the total energy of the simulation block was averaged over several time intervals covering the production stage, and it was checked that these average values followed a normal distribution. Similar tests were made for the pressure inside the block. An additional proof of sufficient relaxation comes from the observations that (i) during the subsequent diffusion runs (see below), the TJ displacements were random and very small (<5 Å) and (ii) the mean-squared atomic displacements accurately followed the Einstein relation. Snapshots containing the atomic coordinates were saved every 0.02 ns and later postprocessed to compute the diffusion coefficients.

The diffusion coefficients D were calculated from the linear fits of $\langle X^2 \rangle$ versus Δt plots using the Einstein relation $D=\langle X^2 \rangle / 2\Delta t$. Here, Δt is the diffusion time and $\langle X^2 \rangle$ is the mean-squared displacement of atoms over the time Δt in the X direction parallel to the TJ. Since the atoms are labeled, $\langle X^2 \rangle$ was computed by comparing the initial and final coordinates of all atoms initially contained within a selected probe region and averaging their squared displacements in X over the time interval between t and $t+\Delta t$. This obtained value of $\langle X^2 \rangle$ was additionally averaged over all choices of the reference time t by increasing it from zero to $t_{\max}-\Delta t$, where $t_{\max}$ is the duration of the entire MD run (10 ns). The maximum diffusion time Δt was chosen to be 1–2 ns, depending on the temperature.

The probe regions selected for GB diffusion were parallelepipeds aligned with the GB planes (Fig. 2), which had the dimensions $L \times W \times 2d$, where $L=66$ Å is the cylinder length. The width $W=35$ Å parallel to the GB was chosen so as to include as large a GB area as possible but avoid the influence of the TJ and the fixed regions. Since our goal was to evaluate the diffusivity in the GB core area, the half thickness of the probe region was $d=5$ Å, which is close to the typical diffusion width of GBs.[15]

For TJ diffusion, the probe region was a cylinder with the radius d placed at the diffusion center of the TJ (Fig. 2). Special care was taken to keep track of the position of the center. To achieve this, a testing MD run was made prior to the production run at each temperature and a group of atoms with the largest magnitude of displacements in X was identified. Such "fastest" atoms were invariably found in the TJ region, which was already a qualitative proof of its enhanced diffusivity. The average coordinates of the fastest atoms were used to select the diffusion center of the TJ. Furthermore, the position of the center was recomputed for each snapshot during the production simulations and it was found to change only by small amounts that did not exceed d. This confirmed the high stability of our TJ geometry. However, the position of the center had to be slightly readjusted for each temperature since changes in the contact angles of the GBs could

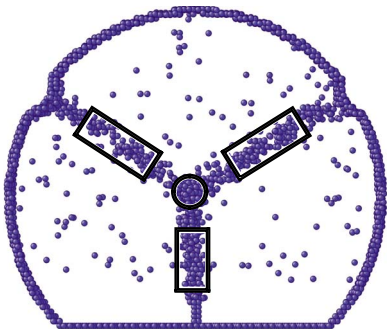

FIG. 2. (Color online) The plot indicates the probe regions chosen for diffusion calculations for the TJ and the GBs. Only atoms with coordination number below a certain bound are shown.

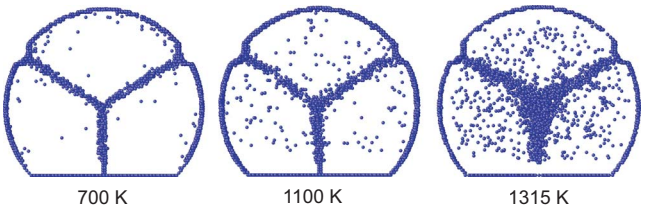

FIG. 3. (Color online) Change in the structure of the GBs and the TJ with temperature. The visualization method is explained in the text. The bulk melting temperature with this interatomic potential is 1327 K.

produce TJ displacements. Diffusion coefficients in liquid copper were computed separately from mean-squared displacements of atoms at several temperatures using a large periodic supercell at zero pressure.

III. RESULTS

The TJ and GB structures were examined after "quenching" from 700 to 0 K. Although the structures contained a number of quenched-in point defects, they were very coherent and had thicknesses on the order of 2 to 3 interatomic distances. These structures remained quite coherent also at finite—but not too high—temperatures. From the dihedral angle of the GBs, the 0 K energy of the GGB is estimated to be approximately 0.9 of the Σ5 GB energy. This number is very reasonable given that the Σ5(210) GB has the highest energy among all boundaries studied in Refs. 16 and 17 and is roughly 10% above the energies of typical high-angle GBs.

Examination of the MD snapshots reveals that the GBs and the TJ become increasingly disordered with temperature, as illustrated in Fig. 3. (The visualization employs the coordination-number mode of the ATOMEYE program,[18] plotting only atoms whose coordination number is smaller than a certain number.) Near the bulk melting point the GBs become increasingly wider, especially in the TJ region, and develop a liquidlike structure. At 1315 K, the TJ essentially turns into a liquid pipe.

Typical $\langle X^2 \rangle$ versus time plots are displayed in Fig. 4. Their linearity demonstrates that the Einstein relation is followed accurately, confirming that we have properly sampled the diffusion regime. The slopes of the curves indicate that the TJ diffusion is faster than diffusion in the Σ5 GB and that both diffusivities increase with temperature.

All diffusion coefficients obtained in this work are summarized in the Arrhenius diagram in Fig. 5. Observe the encouraging agreement with experimental data for self-diffusion in the bulk liquid[19] and high-purity polycrystalline Cu,[20,21] lending confidence to our simulation methodology. Diffusion along the TJ is seen to be faster than diffusion in both GBs at all temperatures tested. Also, the Σ5(210) GB shows a higher diffusivity than the GGB at all temperatures. The latter observation is consistent with the previous work,[10] in which diffusion in the Σ5(210) GB was found to be faster than in the Σ5(310) and Σ17(530) GBs. Note the GB and TJ diffusivities converge at high temperatures and tend to diffu-

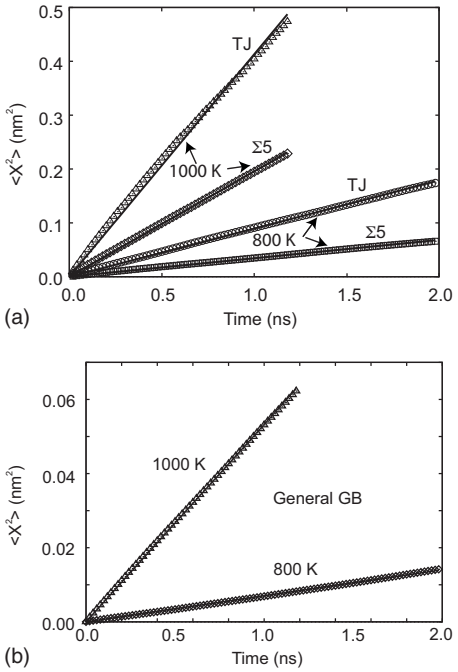

FIG. 4. Typical plots of the mean-squared displacements calculated for (a) the Σ5 GB and the TJ and (b) the general GB at 800 and 1000 K. The lines show the linear fits.

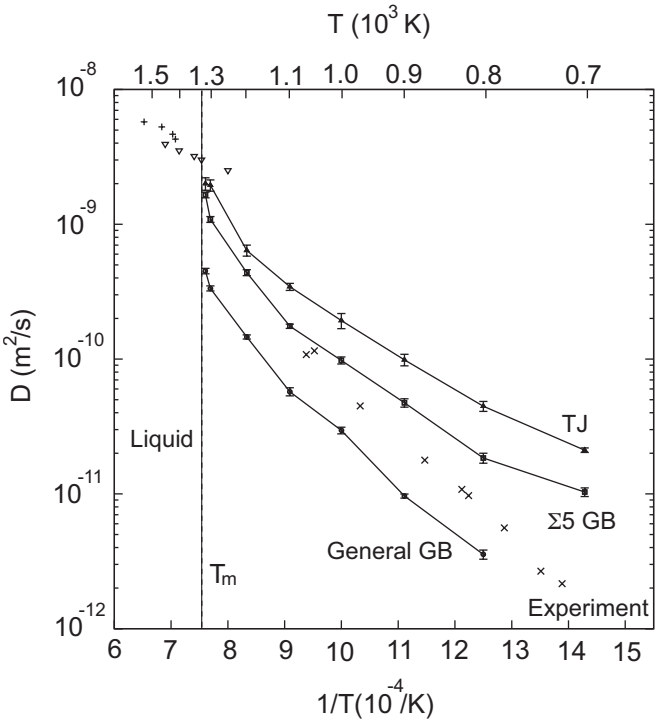

FIG. 5. Arrhenius diagram of diffusion coefficients D calculated for the TJ (△), the Σ5 GB (□), the GGB (○), and liquid copper (▽). The vertical dashed line indicates the melting point of Cu with this embedded-atom potential (1327 K). Experimental data for self-diffusion in liquid copper (Ref. 19) (+) and in high-purity copper polycrystals (Ref. 20) (×) are shown for comparison.

TABLE I. Arrhenius parameters Q (activation energy) and D_0 (pre-exponential factor) of TJ and GB diffusion in Cu obtained in this work. The Arrhenius parameters of lattice self-diffusion computed with the same interatomic potential are given for comparison.

Defect	Q (eV)	D_0 (m^2/s)
Triple junction	0.47 ± 0.02	$(4.3 \pm 1.3) \times 10^{-8}$
$\Sigma 5$ GB	0.48 ± 0.04	$(2.5 \pm 1.4) \times 10^{-8}$
GGB	0.71 ± 0.02	$(1.0 \pm 0.2) \times 10^{-7}$
Perfect lattice	1.961[a]	3.1×10^{-6} [b]

[a]Sum of the vacancy formation and migration energies (Table II in Ref. 16).

[b]Computed from the lattice parameter and the vacancy formation entropy and jump-attempt frequency (Table II in Ref. 16).

sivity of bulk liquid, which is in agreement with the premelting process. To put these data in perspective, the self-diffusion coefficient in the lattice computed with the same embedded-atom method (EAM) potential at the bulk melting point is as low as 1.1×10^{-13} m^2/s, which is beyond the scale of Fig. 5.

Despite the significant scatter of the data points, the Arrhenius plots in Fig. 5 can be linearized except near the melting point. A fit according to the Arrhenius equation $D = D_0 \exp(-Q/kT)$ (k is the Boltzmann factor) in the temperature interval 700–1100 K gives the activation energies Q and pre-exponential factors D_0 summarized in Table I. Although these Arrhenius parameters slightly depend on the choice of the temperature interval, their ordering remains the same. The activation energy of TJ diffusion is always the smallest and close to that of the $\Sigma 5$ GB.

IV. DISCUSSION AND CONCLUSIONS

We have proposed a computational method to create a single equilibrium TJ with controlled crystallographic orientations of the grains. The geometric stability of the TJ is ensured by the fixed boundary conditions which pin the GBs at three points. An alternative procedure could be to prepare three separate wedge-shaped grains with angles that sum to 180° and join them together like a cake. Besides being much more tedious, this approach does not offer an easy way to eliminate the mismatch stresses that may arise due to possible changes in the translational states of the grains during the relaxation. In addition, the free volumes of the GBs and of the TJ would have to be accommodated by elastic stresses. In contrast, in our method the TJ forms *naturally*, as a result of GB migration at a high temperature [Fig. 1(b)]. In this process, the equilibrium atomic density in the GBs and in the TJ can be reached by atomic diffusion to/from the free surface. Although in this paper we have implemented a particular set of grain misorientations shown in Fig. 1, other grain misorientations could have been created as well. A precise control of the GB planes is more difficult, although some control is possible through judicious choices of the dimensions of the initial grains.

The MD simulations indicate that both the GBs and the TJ become increasingly disordered at high temperatures and exhibit a premelting behavior near the bulk melting point (Fig. 3). As the temperature approaches T_m, the premelting first starts at the TJ, then extends to the $\Sigma 5$ GB, and finally occurs at the GGBs. This sequence of premelting processes suggests that the TJ has a higher excess free energy than the GBs studied here. The question of whether TJs carry an excess free energy relative to the adjoining GBs ("excess of excesses") has long been debated in the literature.[11]

Diffusion simulations have been conducted over a wide temperature range and the diffusion coefficients in the TJ and the GBs have been extracted from the mean-squared atomic displacements. It should be mentioned that due to the fixed boundary conditions and conserved number of atoms in the model, the point-defect equilibrium at the diffusion temperature could only be achieved by defect generation and/or absorption at the TJ and the GBs. At high temperatures, the TJ and the boundaries were premelted or at least highly disordered, making them effective sinks and sources of point defects. Even at the lowest temperature studied here (700 K), the TJ region was still fairly disordered and was presumably able to generate and absorb point defects during the prediffusion anneal. This was evidenced by the linearity of the mean-square displacements versus time plots at this temperature, as well as by the independence of the diffusion results on the thermal history. For example, an additional low-temperature anneal of the TJ prior to carving out the cylinder [i.e., when the GBs were still connected to the surface, Fig. 1(b)] did not change the diffusion coefficients within the statistical error. It is important to recognize, however, that low-temperature MD simulations in closed systems containing well-ordered GBs or other extended defects can be associated with nonequilibrium point-defect concentrations and can give inaccurate diffusion coefficients.

Our calculations confirm that diffusion along the TJ is faster than diffusion along the GBs at all temperatures (Fig. 5). Our results also suggest that for diffusion along "typical" GBs, such as the GGB tested here, can be orders of magnitude slower than TJ diffusion at low temperatures. This conclusion is consistent with recent experimental measurements.[5] However, diffusion in the highly energetic $\Sigma 5(210)$ GB is only a factor of 2 slower than in the TJ. Although this small gap tends to slightly increase at low temperatures, Fig. 5 and the Arrhenius parameters (Table I) clearly indicate that high-diffusivity GBs such as $\Sigma 5$ can be more efficient for atomic transport in polycrystals than TJs. The factor of 2 higher diffusivity of TJs is hardly sufficient for making a significant contribution considering their much smaller cross-sectional area in comparison with GBs.

As the temperature approaches the melting point, the TJ and GB diffusivities converge to the bulk liquid diffusivity, reflecting the premelting process. A very similar behavior was recently observed for GB diffusion.[10] The rapid increase in the diffusivity near T_m produces a strong upward curvature of the Arrhenius plots and the concept of activation energy loses its physical significance. From the convergence of the diffusivities at high temperatures, it appears unlikely that TJs can make a sensible contribution to diffusional creep at high temperatures given their relatively small cross-sectional area

even in nanocrystalline materials. With most GBs in nanocrystals being of general type, the contribution to the creep rates often attributed to TJs might be overestimated.

ACKNOWLEDGMENTS

We are grateful to W. J. Boettinger for numerous fruitful discussions. We have benefited greatly from interactions with many colleagues during coordination meetings sponsored by the DOE-BES Computational Materials Science Network (CMSN) program. This work was supported by the U.S. Department of Energy, Office of Basic Energy Sciences. We used the resources of the National Energy Research Scientific Computing Center supported by the Office of Science of the U.S. Department of Energy under Contract No. DE-AC02-05CH11231.

*tfrolov@gmu.edu
†ymishin@gmu.edu

[1] F. A. Mohamed and Y. Li, Mater. Sci. Eng., A **298**, 1 (2001).
[2] M. Xiao and Q. P. Kong, Scr. Mater. **36**, 299 (1997).
[3] Y. Chen and C. A. Schuh, Scr. Mater. **57**, 253 (2007).
[4] R. Kremer, R. Narayanan, S. Shekhar, and A. H. King, J. Mater. Sci. **40**, 2795 (2005).
[5] B. Bokstein, V. Ivanov, O. Oreshina, A. Peteline, and S. Peteline, Mater. Sci. Eng., A **302**, 151 (2001).
[6] K. M. Yin, A. H. King, T. E. Hsieh, F. R. Chen, J. J. Kai, and L. Chang, Microsc. Microanal. **3**, 417 (1997)
[7] L. M. Klinger, L. A. Levin, and A. L. Petelin, Defect Diffus. Forum **143-147**, 1523 (1997).
[8] A. A. Fedorov, M. Y. Gutkin, and I. A. Ovid'ko, Scr. Mater. **47**, 51 (2002).
[9] Y. Mishin, in *Handbook of Materials Modeling*, edited by S. Yip (Springer, Dordrecht, 2005), Chap. 2.2, pp. 459–478.
[10] A. Suzuki and Y. Mishin, J. Mater. Sci. **40**, 3155 (2005).
[11] S. G. Srinivasan, J. W. Cahn, H. Jonsson, and G. Kalonji, Acta Mater. **47**, 2821 (1999).
[12] O. A. Shenderova and D. W. Brenner, Phys. Rev. B **60**, 7053 (1999).
[13] M. Upmanyu, D. J. Srolovitz, L. S. Shvindlerman, and G. Gottstein, Acta Mater. **50**, 1405 (2002).
[14] Y. Mishin, M. J. Mehl, D. A. Papaconstantopoulos, A. F. Voter, and J. D. Kress, Phys. Rev. B **63**, 224106 (2001).
[15] I. Kaur, Y. Mishin, and W. Gust, *Fundamentals of Grain and Interphase Boundary Diffusion* (Wiley, Chichester, 1995).
[16] A. Suzuki and Y. Mishin, Interface Sci. **11**, 131 (2003).
[17] A. Suzuki and Y. Mishin, Interface Sci. **11**, 425 (2003).
[18] J. Li, Modell. Simul. Mater. Sci. Eng. **11**, 173 (2003).
[19] J. Henderson and L. Yang, Trans. Metall. Soc. AIME **221**, 72 (1961).
[20] T. Surholt and Chr. Herzig, Acta Mater. **45**, 3817 (1997).
[21] The GB diffusion coefficients were obtained by dividing the measured products $D\delta$ by the GB diffusion width $\delta = 10$ Å.